



Cite this: *RSC Adv.*, 2017, 7, 24822

A novel long-wavelength fluorescent probe for discrimination of different palladium species based on Pd-catalyzed reactions†

Ting Yu, Guoxing Yin, Peng Yin, * Ying Zeng, Haitao Li, * Youyu Zhang and Shouzhao Yao

We have synthesized a novel long-wavelength fluorescent probe **MFC** for detection of palladium (Pd^0). This probe not only shows high selectivity for palladium, but also could quickly discriminate different palladium species (Pd^0 , Pd^{2+} , Pd^{4+}) in phosphate buffered solution. After the reaction with $\text{Pd}(\text{PPh}_3)_4$, the UV absorption of the probe **MFC** shifts from 334 nm to 594 nm within a few minutes. The probe **MFC** conjugated with alkyl carbamate, which destroys the principle of intramolecular charge transfer (ICT) and shows weak fluorescence. Based on the Pd^0 -catalyzed Tsuji–Trost deallylation reaction, the fluorogen was released and the fluorescence intensity at 612 nm was observed with 13-fold enhancement along with an obvious color change from yellow to purple with low detection limit.

Received 11th February 2017
Accepted 3rd May 2017

DOI: 10.1039/c7ra01731f

rsc.li/rsc-advances

Introduction

Palladium, one of the most important noble transitional metal catalysts, is widely used in organic reactions, medical instruments, fuel crowns, electronics and jewellery.^{1–5} The concern of palladium for human health and environmental contamination is increasing and a lot of attention has been paid to it recently.⁶ In particular, palladium could bind to thiol-containing proteins, DNA, and other biomolecules, causing potential toxicity and carcinogenicity to humans, and it is strongly limited by governmental regulations to 5–10 ppm in end products.^{7–10} Therefore, it is urgently required to develop methods for selective and sensitive monitoring of palladium species in the environment, food and living organisms.

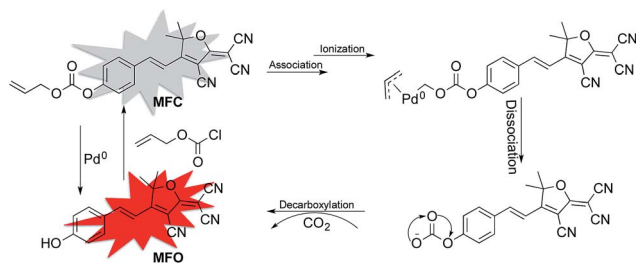
The traditional analytical methods for detecting palladium species are atomic absorption spectroscopy (AAS), inductively coupled plasma mass spectrometry (ICP-MS), inductively coupled plasma optical emission spectrometry (ICP-OES), solid phase micro extraction-high performance liquid chromatography and X-ray fluorescence, which require expensive instruments and well-trained individuals.^{11–14} Recently, fluorescent probes have been widely applied in biological and environmental studies owing to its simple operation, low-cost, high sensitivity and high selectivity.^{15–19} Plenty of fluorescent probes

have been reported for the detection of palladium, most of which were based on the Pd^0 -catalyzed Tsuji–Trost deallylation and depropargylation.^{20–24} Consequently, several fluorescence probes based on intramolecular charge transfer (ICT) and the excited stated intramolecular proton transfer (ESIPT) had been reported. Liu²⁴ *et al.* designed a novel turn-on ratiometric fluorescence probe by ICT, which conducted two-photon fluorescent platform with a rigid oxygen-bridge conformation based on the green fluorescence protein. Zhang²⁵ *et al.* designed a coumarin-based fluorescent probe for the detection of palladium with the detection limit to be 0.34 nM. Also, this probe showed nonfluorescence when connecting with allyl carbonate ester. Wang²⁶ *et al.* synthesized a colorimetric and turn-on fluorescent probe for the detection of palladium with high selectivity and sensitivity, which also used the allyl carbamate as the recognition unit for palladium likewise others. However, some of them still have some limitations including long time reaction times, emission in the short-wavelength region and small Stoke shift, which limits their applications *in vivo*. Therefore, developing some palladium fluorescent probe that could emit in the red or NIR region is of great importance, for the longer wavelength fluorescence could reduce the background interference from the indigenous biomolecules of the living organisms.

2-Dicyano-methylene-3-cyano-4,5,5-trimethyl-2,5-dihydrofuran (TCF) and its derivatives have typical donor– π –acceptor (D– π –A) structure, longer emission wavelength in the red (or NIR) region, which contribute their application in dye-sensitized solar cells, bio-imaging and organic nonlinear optical crystals.^{27–35} Herein, a long-wavelength fluorescent probe (**MFC**) was designed for sensing palladium species, based on the properties of TCF and the principle of intramolecular charge transfer (ICT) (Scheme 1).³⁶

Key Laboratory of Chemical Biology and Traditional Chinese Medicine Research, Ministry of Education, College of Chemistry and Chemical Engineering, Hunan Normal University, Changsha 410081, PR China. E-mail: yinpeng@hunnu.edu.cn; haitaoli@hunnu.edu.cn

† Electronic supplementary information (ESI) available: Structural characterization data, absorption and fluorescence spectra, TLC, ¹H NMR, ¹³C NMR, and HRMS. See DOI: 10.1039/c7ra01731f



Scheme 1 Structure of probe MFC and the proposed mechanism for selective recognition of Pd⁰.

Allyl carbamate group was usually used as the response unit for Pd⁰. After reaction with palladium, the allyl carbamate group would be cleaved from the probe, and substrate with strong fluorescence would be released. The probe MFC showed high sensitivity and selectivity toward palladium and met the requirement of both emitting in the red wavelength region and naked eye detection.

Experimental

Materials and instrumentation

The chemicals and solvents were purchased from Aladdin (Shanghai, China) and used without further purification. Pd(PPh₃)₄, NaCl, KCl, AgNO₃, ZnCl₂, CdCl₂, FeCl₃, CrCl₃, CuCl₂, Hg(NO₃)₂, MnCl₂, PbCl₂, Na₂HPO₄, NaH₂PO₄, Pd(PPh₃)₂Cl₂, (NH₄)₂PdCl₆, (MeCN)₂PdCl₂, NaBH₄ were of analytical grade. TLC analysis was performed using precoated silica plates. UV-vis absorption spectra were collected on a UV-2450 spectrophotometer (Shimadzu Co., Japan). Fluorescence spectra were recorded on Hitachi F-7000 spectrophotometer (Hitachi Ltd, Japan). ¹H NMR and ¹³C NMR spectra were obtained with tetramethyl silane (TMS) as the internal standard on a BRUKER AVANCE-500 spectrometer. IR spectrum was recorded on NEXUS as KBr pellets and were reported in cm⁻¹. HRMS spectrum was recorded on AB TripleTOF 5600+ (U.S AB SCIEX).

Synthesis of compound TCF

Compound TCF was prepared according to the literature method.³⁷ To a mixture of 3-hydroxy-3-methylbutan-2-one (9.00 g, 88.12 mmol), malononitrile (11.92 g, 180.43 mmol) in ethanol (30 mL) was added sodium ethanol (0.90 g, 13.22 mmol), then the mixture was heated to reflux for 2 h until no starting compound was indicated by thin layer chromatography (TLC). After cooled to room temperature, the mixture was filtered and washed with cooled ethanol three times. The residue was dried under vacuum to give 15.00 g (85.71%) of TCF as gray solid. ¹H NMR (500 MHz, chloroform-*d*) δ: 2.39 (s, 3H), 1.65 (s, 6H). ¹³C NMR (126 MHz, chloroform-*d*) δ: 182.7, 175.2, 111.0, 109.0, 104.8, 99.8, 58.4, 24.4, 14.2.

Synthesis of MFO

A mixture of TCF (0.60 g, 3.01 mmol) and 4-hydroxybenzaldehyde (0.38 g, 3.10 mmol) in ethanol (20 mL) was heated to reflux until

compound TCF had been consumed, which was monitored by TLC. After cooled to room temperature, the mixture was filtered and washed with cooled ethanol three times. The residue was dried under vacuum to give 0.80 g (88.88%) pure product of MFO as red solid. ¹H NMR (500 MHz, DMSO-*d*₆) δ: 10.62 (s, 1H), 7.91 (d, *J* = 16.1 Hz, 1H), 7.81 (d, *J* = 8.3 Hz, 2H), 7.02 (d, *J* = 16.2 Hz, 1H), 6.91 (d, *J* = 8.3 Hz, 2H), 1.78 (s, 6H). ¹³C NMR (126 MHz, DMSO-*d*₆) δ: 177.7, 176.3, 162.8, 148.8, 132.8, 126.2, 116.9, 113.4, 112.6, 112.2, 111.7, 99.5, 97.0, 53.7, 25.8 ppm.

Synthesis of probe MFC

Compound MFO (0.60 g, 1.98 mmol) was dissolved in anhydrous acetonitrile and cooled to 0 °C by ice-water bath. Then allyl chloroformate (0.24 mL, 2.19 mmol) and a few drops of redistilled triethylamine were added to the solution under stirring. The reaction mixture was stirred for 1 h and warmed to room temperature. After quenched by adding 10 mL water, the mixture was extracted with dichloromethane for three times. The combined organic layers were dried over anhydrous Na₂SO₄. The solvent was filtered, and dried under vacuum to yield the brown solid (704 mg, 91.87%). ¹H NMR (500 MHz, chloroform-*d*) δ: 7.76–7.69 (m, 2H), 7.67 (d, *J* = 16.4 Hz, 1H), 7.41–7.34 (m, 2H), 7.02 (d, *J* = 16.4 Hz, 1H), 6.03 (ddt, *J* = 16.5, 10.4, 5.9 Hz, 1H), 5.48 (dq, *J* = 17.2, 1.4 Hz, 1H), 5.39 (dd, *J* = 10.4, 1.3 Hz, 1H), 4.79 (dt, *J* = 5.9, 1.4 Hz, 2H), 1.83 (s, 6H). ¹³C NMR (126 MHz, chloroform-*d*) δ: 173.5, 154.1, 152.6, 145.9, 131.6, 130.8, 130.3, 122.2, 120.0, 115.1, 111.5, 110.7, 110.1, 100.4, 97.8, 69.6, 26.4 ppm. IR (cm⁻¹) 3070, 3046, 2994, 2965, 2748, 2417, 2177, 1765, 1580, 1621, 1378, 1309, 950, 858, 774. HRMS (FTMS ESI⁺): *m/z* calcd for C₂₂H₁₇N₃O₄ 386.1141 [M-H]⁺; found 386.1122.

General procedure for fluorescence and UV-visible measurements

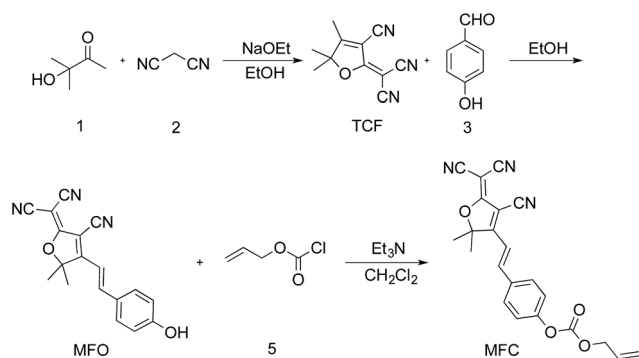
UV-vis absorption and fluorescence spectra studies were conducted in a mixture solution of DMSO/PBS (10 mM, pH = 7.4, 3 : 7, v/v). A volume of 2.0 mL of the solution containing probe MFC (25 μM for UV-vis absorption and 10 μM for fluorescence experiments) was first introduced to a quartz cell, following additions of 10 μL of Pd(PPh₃)₄ stock solution (10 mM). The kinetic investigations were carried out by measuring fluorescence intensities of the resulting mixture at different time intervals. The fluorescence intensities were recorded with an excitation wavelength of 560 nm and emission wavelength ranging from 580 nm to 700 nm. Both the excitation and emission slit was set as 5.0 nm. The responses of interferences were performed by adding 4 equiv. of different anions and palladium-containing compounds (20 μM) to each sample. PBS buffers with different pH values were chosen for investigation the effect of pH. The limit of detection (LOD) was determined by adding Pd(PPh₃)₄ over a series of concentrations into the probe MFC samples.

Results and discussion

Probe design and synthesis

The probe MFC was prepared conveniently according to the synthetic routine in Scheme 2. Firstly, the compound TCF was





Scheme 2 Preparation of probe MFC.

prepared by the 3-hydroxy-3-methylbutan-2-one and malononitrile in ethanol and sodium ethanol. Next, the compound TCF and 4-hydroxybenzaldehyde was heated to reflux in ethanol, yielding the product MFO. Finally, the probe MFC was synthesized from MFO and allyl chloroformate with a satisfactory yield. The detailed characterizations of the intermediates and probe MFC are shown in the ESI (Fig. S5–S11 in ESI†).

The optical property and sensing potential of MFC

The spectral properties of probe MFC were initially investigated in the absence and presence of Pd⁰ in a mixture solution of DMSO and PBS (pH = 7.4, v/v 3 : 7). Pd(PPh₃)₄ was used as the resource of Pd⁰ in all of the experiments. The free probe MFC exhibits a major UV absorption at 334 nm as shown in Fig. 1a. However, after treated with 2.0 equiv. of Pd(PPh₃)₄, a remarkable change in the absorption spectrum was obtained and a high absorption peak was observed at 594 nm (Fig. 1a). Meanwhile, marked color changes of the solution were obviously noticed from yellow to purple in visible light, which could enable the naked-eye visual detection of Pd⁰ (inset Fig. 1a). Consistently, in the fluorescence spectra, probe MFC exhibited very weak fluorescence at 612 nm as expected when excited at 560 nm, and a dramatic turn-on fluorescence enhancement at 612 nm was observed after triggered with Pd(PPh₃)₄ (Fig. 1b). Correspondingly, a notable colour change from bright blue to green was observed by naked eye when excited at 365 nm by handheld UV lamp (Fig. 1b inset).

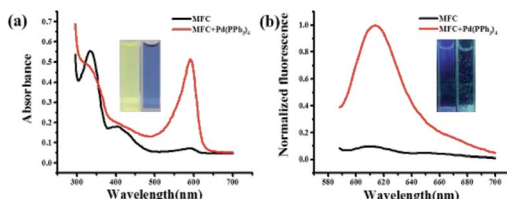


Fig. 1 (a) The absorption spectra and (b) the fluorescence spectra of probe MFC (25 μM) and probe MFC with 2 equiv. of Pd(PPh₃)₄ at 37 °C in DMSO/PBS buffer (10 mM, pH = 7.4, 3 : 7, v/v). λ_{Ex} = 560 nm, λ_{Em} = 612 nm. Inset image: (a), left: visible-light of 10 μM probe, right: 10 μM probe with 20 μM Pd(PPh₃)₄; (b), left: fluorescence image of 10 μM probe, right: 10 μM probe with 20 μM Pd(PPh₃)₄.

The effect of the ratio of DMSO : PBS (pH = 7.4) was also investigated (Fig. S1 in ESI†). And the best ratio of DMSO/PBS (pH = 7.4) was found to be 3 : 7. Furthermore, normally used buffer solutions (PBS, HEPES and Tris–HCl) were also tested for the probe MFC and the mixture of probe MFC with Pd(PPh₃)₄. Judging from the results, the buffer solution of PBS exhibited the best results (Fig. S2 in ESI†). Therefore, the following experiments were carried out in the solution of DMSO/PBS (3 : 7, v/v). Encouraged by these observations, the time-dependent fluorescence intensity changes of probe MFC in presence of Pd(PPh₃)₄ was studied (Fig. S3 in ESI†). Firstly, the stability experiments of the probe MFC at pH 7.4 was investigated. Encouragingly, the probe MFC has little hydrolysis under pH 7.4 for 1 h (Fig. S3a in ESI†). While, upon addition of 2.0 equiv. of Pd(PPh₃)₄ to the probe solution, an initial fast, followed by gradual increase of the fluorescent intensity was obviously observed, and it came to a plateau in about 20 min. Furthermore, the reaction of the probe MFC and Pd⁰ could be easily detected by TLC plate and most of the probe had been consumed after reacted with Pd(PPh₃)₄ for 20 min (Fig. S4 in ESI†).

Effect of pH

With respect to the pH effect, as is well known, the carbonate group is sensitive to pH change and easily hydrolyzed under both acidic and basic media conditions. We examined the pH effect on probe MFC in the absence and presence of Pd(PPh₃)₄, respectively (Fig. 2). The probe was stable in a pH range of 2.0–6.0 monitored at 612 nm. Fluorescence intensity changed little when pH value range 6.0–7.5. Once the probe was incubated with Pd(PPh₃)₄ within the pH value range 7.0–10.0, fluorescence intensity changed distinctly. These results indicated the response of probe MFC to Pd⁰ were favorable at pH range from 7.0–8.0 including the physiological conditions and the probe could be available for Pd⁰ detection in living organism.

The sensitivity of probe MFC for palladium

The capability of probe MFC for recognizing Pd⁰ was investigated by monitoring fluorescent intensities after adding different concentrations of Pd(PPh₃)₄ under the optimal conditions. The fluorescence intensities at 612 nm increased gradually with the

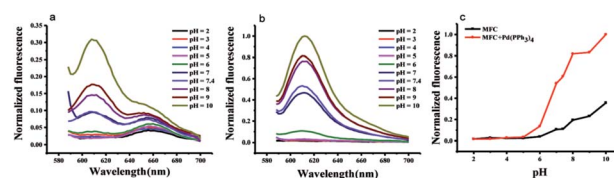


Fig. 2 (a) pH-dependent normalized fluorescence intensity spectrum of free probe MFC (10 μM) in DMSO-PBS buffer (10 mM). (b) pH-dependent normalized fluorescence intensity spectrum of probe MFC (10 μM) with Pd(PPh₃)₄ (20 μM) in DMSO-PBS buffer (10 mM). λ_{Ex} = 560 nm, λ_{Em} = 612 nm. (c) pH effect on the normalized fluorescence intensity spectrum of free probe MFC (10 μM, black line) and probe MFC (10 μM) with Pd(PPh₃)₄ (20 μM, red line) in DMSO-PBS buffer (10 mM). λ_{Ex} = 560 nm, λ_{Em} = 612 nm.



increase of the concentration of $\text{Pd}(\text{PPh}_3)_4$ (Fig. 3). A good linearity of the fluorescence intensity at 612 nm *versus* the concentration of $\text{Pd}(\text{PPh}_3)_4$ from 0 to 2.0 μM was obtained with the detection limit as 1.4 nM ($R^2 = 0.99356$). And only 0.2 equiv. Pd^0 could consume most of the probe **MFC** after 20 min. Owing to the specific properties of palladium, probe **MFC** displayed a high sensitivity toward Pd^0 . The results indicated that a free product MFO was generated by the palladium-triggered reaction, which could indirectly be confirmed by thin layer chromatography (TLC) (Fig. S4 in ESI†).

The selectivity of probe **MFC** for palladium

To illustrate the good selectivity of this novel probe to Pd^0 , a series of metal ions were evaluated. As shown in Fig. 4a, only the addition of Pd^0 induced remarkable fluorescence increase. In contrast, nearly no or little fluorescence changes were observed in the presence of Fe^{3+} , Mg^{2+} , Cd^{2+} , Co^{2+} , Ba^{2+} , Ni^+ , Cu^{2+} , Ag^+ , Al^{3+} , Ca^{2+} , Li^+ , Zn^{2+} , Mn^{2+} , Hg^{2+} and Ti^{3+} . Competitive experiments involving the impacts of above mentioned metal ions in the detection of Pd^0 were performed, which indicated the addition of various metal ions had a negligible effect on the Pd^0 detection (Fig. 4b). These results demonstrated that the probe **MFC** showed an excellent selectivity to Pd^0 over other competitive metal ions, which should be attributed to the specific Pd^0 -triggered reactions.

The selectivity of probe **MFC** for different palladium

The reactivities of probe **MFC** towards other oxidation states of palladium metal sources, such as PbCl_2 , $(\text{MeCN})_2\text{PdCl}_2$, $\text{Pd}(\text{PPh}_3)_2\text{Cl}_2$, $(\text{NH}_4)_2\text{PdCl}_6$, were also examined. The addition of Pd^{2+} and Pd^{4+} to the solution of probe **MFC** had little fluorescence change even with long times (Fig. 4c). While, after the addition of micromolar NaBH_4 , similar responses to probe **MFC** as Pd^0 were obtained, which meant that $\text{Pd}^{2+}/\text{Pd}^{4+}$ species could be reduced to Pd^0 (Fig. 4d). That meant probe **MFC** could recognize the palladium species in all of the typical oxidation states and discriminate Pd^0 from $\text{Pd}^{2+}/\text{Pd}^{4+}$ under different test conditions. These results demonstrated that probe **MFC** could be employed for specific recognition of Pd^0 species.

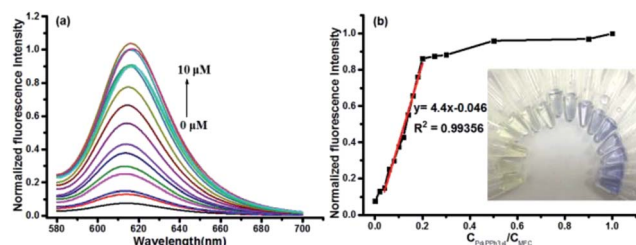


Fig. 3 (a) Normalized fluorescence intensity spectra of probe **MFC** (10 μM) upon addition of increasing concentrations of $\text{Pd}(\text{PPh}_3)_4$ (0–10 μM) in DMSO-PBS buffer (10 mM, pH 7.4, 3 : 7, v/v). $\lambda_{\text{Ex}} = 560 \text{ nm}$, $\lambda_{\text{Em}} = 612 \text{ nm}$. (b) The linear relationship between the fluorescence intensity of probe **MFC** (10 μM) at 612 nm and the concentrations of $\text{Pd}(\text{PPh}_3)_4$ (0–10 μM) in DMSO-PBS buffer (10 mM, pH 7.4, 3 : 7, v/v).

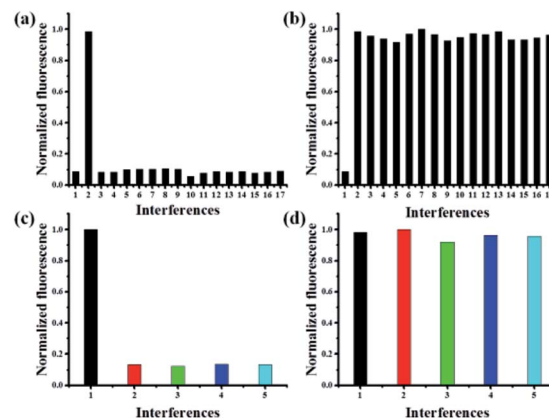


Fig. 4 (a) Normalized fluorescence intensity of probe **MFC** (10 μM) and (b) probe **MFC** (10 μM) with $\text{Pd}(\text{PPh}_3)_4$ (20 μM) in the presence of 40 μM of different interferences in DMSO-PBS buffer (10 mM, pH = 7.4): (1) blank, (2) $\text{Pd}(\text{PPh}_3)_4$, (3) FeCl_3 , (4) MgCl_2 , (5) CdCl_2 , (6) CoCl_2 , (7) BaCl_2 , (8) NiCl_2 , (9) CuCl_2 , (10) AgNO_3 , (11) AlCl_3 , (12) CaCl_2 , (13) LiCl , (14) ZnCl_2 , (15) MnCl_2 , (16) $\text{Hg}(\text{NO}_3)_2$, (17) TiCl_3 . (c) Normalized fluorescence intensity of probe **MFC** (10 μM) in the presence of 20 μM of different palladium-containing compound (20 μM) with NaBH_4 at trace concentration [except $\text{Pd}(\text{PPh}_3)_4$] in DMSO-PBS buffer (10 mM, pH = 7.4), $\lambda_{\text{Ex}} = 560 \text{ nm}$, $\lambda_{\text{Em}} = 612 \text{ nm}$. (1) $\text{Pd}(\text{PPh}_3)_4$, (2) $\text{Pd}(\text{PPh}_3)_2\text{Cl}_2$, (3) $(\text{NH}_4)_2\text{PdCl}_6$, (4) $(\text{MeCN})_2\text{-PdCl}_2$, (5) PdCl_2 .

Mechanism

According to previously reported probes with an allyoxy allyloxycarbonyl group for the sensing of Pd^0 , it is proposed that the trigger moiety of the allyl chloroformate unit is initially conjugated with palladium and ionized to form **MFC**- Pd^0 complex and further dissociates π -allylpalladium(II) to produce (*E*)-4-(2-(4-cyano-5-(dicyanomethylene)-2,2-dimethyl-2,5-dihydrofuran-3-yl)vinyl)phenyl carbonate, then decarboxylates to produce the compound MFO (Scheme 1).³⁸ which was further verified by the ^1H NMR spectra for the probe **MFC** and the mixture of the probe **MFC** with $\text{Pd}(\text{PPh}_3)_4$ in deuterated reagents (Fig. 5). The chemical shifts of Ha (Hb), Ha' (Hb') in compound MFO and **MFC** are 7.79 (6.89) ppm and 8.02 (7.42) ppm, respectively. When probe **MFC** was treated with $\text{Pd}(\text{PPh}_3)_4$, it was clearly observed that new peaks attributed to Ha and Hb was generated. Moreover, HRMS analyses also indicated that the free MFO was produced during the detection process (Fig. S12 in ESI†).

Cell fluorescence imaging

Those above findings were encouraging to explore the possibility of using probe **MFC** for intracellular sensing of Pd^0 in living cells, which was conducted using HEK293 cells. The cells were purchased from China Center for Type Culture Collection (Wuhan, China). As shown in Fig. 6c, free probe **MFC** exhibited almost no fluorescence signal, which was consistent with the above fluorescence studies. Contrastingly, after incubation with Pd^0 for 30 min, a strong fluorescence response could be observed (Fig. 6b). The results demonstrated that probe **MFC** is



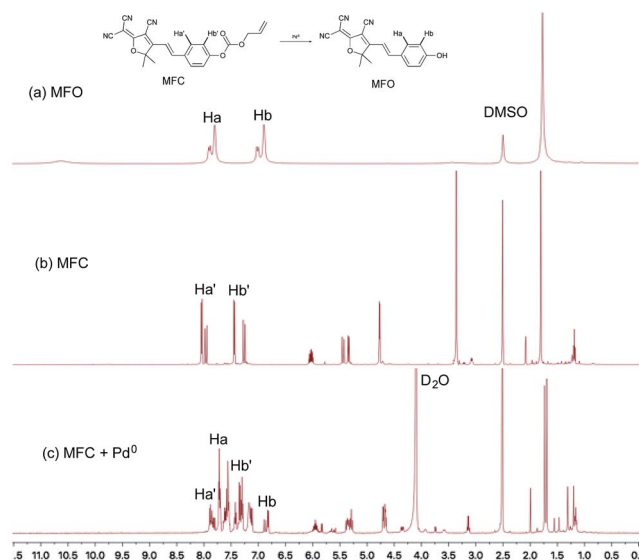


Fig. 5 ^1H NMR spectra of (a) compound MFO in $\text{DMSO}-d_6$ and (b) probe MFC in $\text{DMSO}-d_6$ and (c) probe MFC upon addition of 2 equiv. of $\text{Pd}(\text{PPh}_3)_4$ in $\text{DMSO}-d_6$ and D_2O .

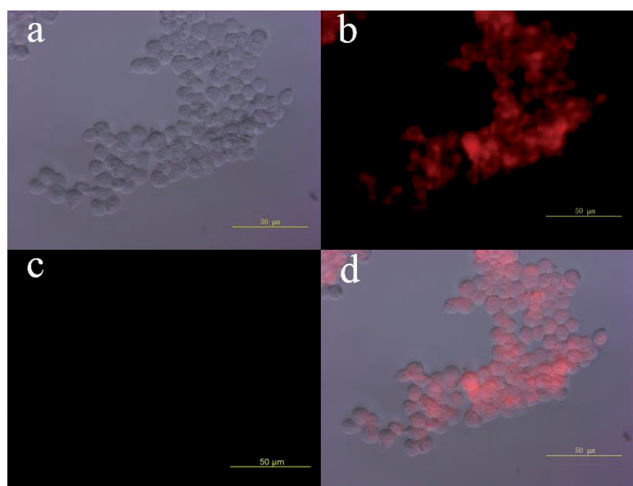


Fig. 6 Fluorescence images of Pd^0 detection in HEK293 cells. (a) Brightfield image of cells incubated with $10.0\ \mu\text{M}$ probe MFC for 60 min and then treated with $20\ \mu\text{M}$ Pd^0 for 30 min at $37\ ^\circ\text{C}$. (b) Fluorescence images of cells in pane (a). (c) Fluorescence image of cells treated with only probe MFC ($10.0\ \mu\text{M}$) for 60 min. (d) Overlay image of (a) and (b).

both cell-permeable and capable of detecting palladium in living cells, which contributes it as a versatile tool for the detection of palladium species in living cells and environmental samples.

Conclusions

In summary, a novel long-wavelength fluorescent probe MFC for discrimination of different palladium species based on Pd^0 -catalyzed reactions was reported, which exhibited high sensitivity and excellent selectivity towards Pd^0 over other

competitive metal ions. The excellent selectivity is due to the highly specific Pd^0 -triggered cleavage process and the long wavelength emission fluorescence should be attributed to the substrate preference and the principle of intramolecular charge transfer. Probe MFC responds totally different to the different oxidation states of palladium species, and have short response times and low detection limit towards Pd^0 species. This strategy would provide a new opportunity for fluorescent sensing of palladium species with the emission in the red range and high selectivity.

Acknowledgements

This work was supported by the funding from the National Natural Science Foundation of China (Grant No. 21405043, 21675051, 21375037 and 21205038) and the Hunan Natural Science Foundation (13JJ2022).

Notes and references

- 1 G. Zeni and R. C. Larock, *Chem. Rev.*, 2004, **104**, 2285–2309.
- 2 T. W. Lyons and M. S. Sanford, *Chem. Rev.*, 2010, **110**, 1147–1169.
- 3 R. Jana, T. P. Pathak and M. S. Sigman, *Chem. Rev.*, 2011, **111**, 1417–1492.
- 4 S. MacQuarrie, J. H. Horton, J. Barnes, K. McEleney, H.-P. Looock and C. M. Crudden, *Angew. Chem., Int. Ed.*, 2008, **47**, 3279–3282.
- 5 D.-G. Cho and J. L. Sessler, *Chem. Soc. Rev.*, 2009, **38**, 1647–1662.
- 6 R. R. Barefoot, *TrAC, Trends Anal. Chem.*, 1999, **18**, 702–707.
- 7 J. Kielhorn, C. Melber, D. Keller and I. Mangelsdorf, *Int. J. Hyg. Environ. Health*, 2002, **205**, 417–432.
- 8 K. Leopold, M. Maier, S. Weber and M. Schuster, *Environ. Pollut.*, 2008, **156**, 341–347.
- 9 C. D. Spicer, T. Triemer and B. G. Davis, *J. Am. Chem. Soc.*, 2012, **134**, 800–803.
- 10 R. M. Yusop, A. Unciti-Broceta, E. M. V. Johansson, R. M. Sanchez-Martin and M. Bradley, *Nat. Chem.*, 2011, **3**, 239–243.
- 11 T. A. Kokya and K. Farhadi, *J. Hazard. Mater.*, 2009, **169**, 726–733.
- 12 K. Van Meel, A. Smekens, M. Behets, P. Kazandjian and R. Van Grieken, *Anal. Chem.*, 2007, **79**, 6383–6389.
- 13 B. Dimitrova, K. Benkhedda, E. Ivanova and F. Adams, *J. Anal. At. Spectrom.*, 2004, **19**, 1394–1396.
- 14 L. Duan, Y. Xu and X. Qian, *Chem. Commun.*, 2008, **47**, 6339–6341.
- 15 A. P. de Silva, H. Q. N. Gunaratne, T. Gunnlaugsson, A. J. M. Huxley, C. P. McCoy, J. T. Rademacher and T. E. Rice, *Chem. Rev.*, 1997, **97**, 1515–1566.
- 16 H. M. Kim and B. R. Cho, *Chem. Rev.*, 2015, **115**, 5014–5055.
- 17 Y. Yang, Q. Zhao, W. Feng and F. Li, *Chem. Rev.*, 2013, **113**, 192–270.
- 18 J. Zhou and H. Ma, *Chem. Sci.*, 2016, **7**, 6309–6315.
- 19 J. Du, M. Hu, J. Fan and X. Peng, *Chem. Soc. Rev.*, 2012, **41**, 4511–4535.



- 20 W. Su, B. Gu, X. Hu, X. Duan, Y. Zhang, H. Li and S. Yao, *Dyes Pigm.*, 2017, **137**, 293–298.
- 21 J.-w. Yan, X.-l. Wang, Q.-f. Tan, P.-f. Yao, J.-h. Tan and L. Zhang, *Analyst*, 2016, **141**, 2376–2379.
- 22 K. Xiang, Y. Liu, C. Li, B. Tian and J. Zhang, *RSC Adv.*, 2015, **5**, 52516–52521.
- 23 J. Qin, X. Li, Z. Chen and F. Feng, *Sens. Actuators, B*, 2016, **232**, 611–618.
- 24 W. Luo and W. Liu, *J. Mater. Chem. B*, 2016, **4**, 3911–3915.
- 25 Y. Liu, K. Xiang, M. Guo, B. Tian and J. Zhang, *Tetrahedron Lett.*, 2016, **57**, 1451–1455.
- 26 M. Liu, T. Leng, K. Wang, Y. Shen and C. Wang, *J. Photochem. Photobiol., A*, 2017, **337**, 25–32.
- 27 Y. Yang, J. Liu, H. Xiao, Z. Zhen and S. Bo, *Dyes Pigm.*, 2017, **139**, 239–246.
- 28 Y. J. Wang, Y. Shi, Z. Wang, Z. Zhu, X. Zhao, H. Nie, J. Qian, A. Qin, J. Z. Sun and B. Z. Tang, *Chem.–Eur. J.*, 2016, **22**, 9784–9791.
- 29 Y.-R. Wang, L. Feng, L. Xu, Y. Li, D.-D. Wang, J. Hou, K. Zhou, Q. Jin, G.-B. Ge, J.-N. Cui and L. Yang, *Chem. Commun.*, 2016, **52**, 6064–6067.
- 30 C. Li, M. Li, Y. Li, Z. Shi, Z.-J. Li, X. Wang, J. Sun, J. Sun, D. Zhang and Z. Cui, *J. Mater. Chem. C*, 2016, **4**, 8392–8398.
- 31 H.-R. Kim, R. Kumar, W. Kim, J. H. Lee, M. Suh, A. Sharma, C. H. Kim, C. Kang and J. Seung Kim, *Chem. Commun.*, 2016, **52**, 7134–7137.
- 32 H. Wang, Y. Yang, J. Liu, F. Liu, L. Qiu, X. Liu and Z. Zhen, *Mater. Lett.*, 2015, **161**, 674–677.
- 33 M.-Y. Wu, K. Li, C.-Y. Li, J.-T. Hou and X.-Q. Yu, *Chem. Commun.*, 2014, **50**, 183–185.
- 34 M. K. Lee, J. Williams, R. J. Twieg, J. Rao and W. E. Moerner, *Chem. Sci.*, 2013, **4**, 220–225.
- 35 J. Wu, S. Bo, J. Liu, T. Zhou, H. Xiao, L. Qiu, Z. Zhen and X. Liu, *Chem. Commun.*, 2012, **48**, 9637–9639.
- 36 L. Feng, Z.-M. Liu, L. Xu, X. Lv, J. Ning, J. Hou, G.-B. Ge, J.-N. Cui and L. Yang, *Chem. Commun.*, 2014, **50**, 14519–14522.
- 37 D. Villemin and L. Liao, *Synth. Commun.*, 2001, **31**, 1771–1780.
- 38 W. Luo and W. Liu, *Dalton Trans.*, 2016, **45**, 11682–11687.

